Bot. Bull. Acad. Sin. (2005) **46:** 205-215

Study on laminar hydathodes of *Ficus formosana* (Moraceae) I. Morphology and ultrastructure

Chyi-Chuann CHEN and Yung-Reui CHEN*

Institute of Molecular and Cellular Biology, National Taiwan University, Taipei, Taiwan

(Received November 15, 2004; Accepted February 22, 2005)

Abstract. In this study, the clearing method, LM, SEM, and TEM were used to examine the morphology and ultrastructures of laminar hydathodes of *Ficus formosana* Maxim. f. *Shimadai* Hayata. Morphologically, the laminar-hydathode of *F. formosana* is complex epithemal type, consisting of water pores, tracheid-ends, epithem cells, and a bounding sheath layer. Water pores are made up of two guard cells, and their pores open permanently. Ultrastructural and cytological data demonstrated that the epithem cell has a dense cytoplasm, numerous mitochondria, an extended ER system, and many small vesicles derived from Golgi bodies. It has proliferate peroxisomes, and their numbers increase with the maturation and aging of the epithem. In addition, abundant plasmodesmata were observed on the contacted cell wall between epithem cells. Variable structures of plasmalemmasome were also observed on the plasma membrane of the epithem. Plasmalemmasome is the result of endocytosis caused by the plasmolysis-deplasmolysis cycle, which is induced by repeating transpiration and guttation day and night. We suggest that the hydathode is an ideal system for studying endocytosis in plants.

Keywords: Endocytosis; Epithem; *Ficus formosana* Maxim. f. *Shimadai* Hayata; Laminar hydathodes; Plasmalemmasome; Ultrastructure; Water pores.

Introduction

Guttation is the process by which water exudes from a leaf surface. It differs from transpiration, in which water passes through the stomata in gas form. Guttation is observed in a wide range of vascular plants and ferns. The hydathode is the apparatus of guttation that consists of stomata-like pores in the epidermis and the epithem, which has a large chamber with masses of thin-wall parenchyma cells and a sheath layer surrounding its tissues (Kramer, 1945). In the early studies of hydathodes, Haberlandt (1914) and Lepschkin (1923) divided them into epidermal and epithemal hydathodes. In the former, water secretion is dependent on the metabolic activity of the specialized epidermal cells on the adaxial surface of leaves near the end of the veins, and this is regarded as an active process. For epithemal hydathodes, on the other hand, the process is passive. They respond directly with the water-conducting system of the plant. The water passing through water pores can be observed when the "root pressure" reaches a certain threshold, as a result of an inhibited or a reduced transpiration.

Hydathodes have been found in different dicot families, including Asteraceae (Lersten and Curtis, 1985), Begoniaceae (Brouillet et al., 1987), Rosaceae (Lersten and Curtis, 1982), Balsaminaceae (Elias and Gelband, 1977), Salicaceae (Curtis and Lersten, 1974), Urticaceae (Smith and Watt, 1986; Lersten and Curtis, 1991), Crassulaceae (Rost, 1969), and Moraceae (Lersten and Peterson, 1974), as well as in cereal plants (Maeda and Maeda, 1987, 1988; Dieffenbach et al., 1980) and pteridophytes (Sperry, 1983). Most of the hydathodes can be found at the tip, on the margin, and/or over the entire surface of leaf. In a small number of species, hydathodes are found on leaf hypodermis (Fahn, 1979). In a few cases, they can also be found in other organs. For example, hydathode is found on the grape tendril (*Vitis vinifera*) (Tucker and Hoefert, 1968). They are also found in certain submerged aquatic plants (Pedersen et al., 1997).

The current study focuses on a particular type of hydathode, the so-called "laminar hydathodes." To our knowledge, three dicot families—i.e., Moraceae, Urticaceae, and Crassulaceae—have this type hydathode distribution (Lersten and Curtis, 1991). On the hydathodes of *Ficus*, in Moraceae, little data have ever been published. For example, Molisch (1916) described the anatomy of the hydathode in *F. javanica*, and Lersten and Peterson (1974) later illustrated the structure of hydathodes in *F. diversifolia* using light microscopy. A detailed investigation into the ultrastructure of the laminar hydathodes in *Ficus* has not yet been completed. The aims of this study were to present the ultrastructural data of the adaxial-laminar hydathodes in *F. formosana* Maxim. f. *Shimadai* Hayata through the clearing method, light microscopy, scanning electron microscopy, and transmission electron microscopy. It is intended to serve as a platform for further studies on the function of laminar hydathodes.

*Corresponding author. Fax: 02-3366-2478; E-mail: yrc@ntu.edu.tw

Materials and Methods

Plant Material

Ficus formosana Maxim. f. *Shimadai* Hayata were planted in soil pots within the greenhouse of the Department of Botany, National Taiwan University. Daily watering, the recording of temperature and humidity by using an automatic device, and the addition of fertilizer at regular intervals were performed consistently through the entire experiment. At the earlier and mature developmental stages, leaves were chosen and harvested for light and electron microscopic studies. We obtained 190 mature leaves from 15 shoots, and data on leaf length and hydathode number on each leaf were recorded.

Light Microscopy (LM)

Mature leaf samples of *F. formosana* Maxim. f. *Shimadai* Hayata containing achlorophyll hydathodes were fixed with 2.5% glutaraldehyde in 0.1 M sodium cacodylate buffer with pH 7.0 for 4 h at room temperature, and then washed in a rinse buffer of 0.1 M sodium cacodylate. The materials were later fixed by 1% OsO_4 in 0.1 M cacodylate buffer at pH 7.0 for 4 h at room temperature, then washed in 0.1 M sodium cacodylate buffer, dehydrated in a gradient acetone series and embedded in Spurr's resin (Spurr, 1969). Resin-embedded samples in rubber mold were polymerized at 70°C for 8 h.

For light microscopy, semithin sections with thickness of 1 μm were cut with glass knives on Ultracut E ultramicrotome and stained with 1% toludine blue. The sections were examined under Zeiss Photomicroscope III and photographed with Kodak TMAX 100.

Transmission Electron Microscopy (TEM)

Ultrathin sections 90 nm thick were cut with a diamond knife and picked up on 75-mesh grid. Then, the section-mounted grids were stained with saturated aqueous uranyl acetate for 25 min, followed by lead citrate for 5 min. The stained sections were observed and photographed under a Hitachi H-600 transmission electron microscope at 75kV.

Scanning Electron Microscopy (SEM)

After fixation and buffer washings were performed as described above, the samples were dehydrated by a series of 100% ethanol rinsing, followed by a final 100% acetone. After drying by a critical point dryer (HITACHI Critical Point Dryer HCP-2), the samples were mounted on aluminum stabs with silver paste. Finally, the samples were coated with palladium-gold in an ion coater (Eiko Engineering, Ltd. IB-2 ion coater) and viewed in a Hitachi S-520 SEM.

Cleaning Method

Venation of translucent leaves was studied using the technique of Shobe and Lersten (1967). Leaves were first cut into pieces of 2 × 1 cm^2. Then, a depigmentation of the chloroplast was performed by placing the samples in 70% ethanol over a water bowl and boiling for 10-30 min. Later, the samples were immersed in 5% aqueous sodium hydroxide at 60°C until the leaf segments became partially translucent. Lactic acid followed in the treatment to make the leaf segments completely translucent.

Results

Morphology of Hydathodes

The leaf of *F. formosana* Maxim. f. *Shimadai* Hayata is narrow and lanceolate to linear in shape. Their laminar hydathodes are distributed on the adaxial surface of the leaves by a scattering arrangement in one linear row between the margin and the mid-rib with extension from the leaf base to the tip (Figure 1A). From a top view, the color of hydathodes in young leaves appears translucent, becoming white at maturity. At the oldest stage of the leaf, they appear brown. Figure 1B shows a mature hydathode, a shallow and colorless circular depression on the adaxial surface of leaf. The epidermis of the hydathode features a group of water pores and epidermal cells, and a giant trichome.

In general, the occurrence of hydathodes is associated with venation. In cleared leaves, hydathodes are located on meshworks of major and minor veins with several free vein-ends. In some cases, they join together and form a junction, with each involving three or more vascular bundles. Figure 1C shows three hydathodes and several tracheid-ends associated together in all directions under them. These laminar hydathodes are of the epithemal type.

A laminar hydathode consists of epidermis and water pores accompanied by a giant trichome and many salt-glan-

→

Figures 1A-I. External features of the laminar hydathodes in *F. formosana* Maxim. f. *Shimadai* Hayata. A, Hydathodes on the adaxial surface of leaf and scattered in a linear arrangement between mid-rib and leaf margin. White points indicate hydathodes. B, Magnification of a hydathode in Figure 1A. Hydathode (arrowhead) consists of a trichome and a group of water pores on leaf upper epidermis. C, Clearing leaf showing the venation pattern and three hydathodes, which is associated with vein-end junctions of the venation (arrowheads). D, SEM micrograph of a young leaf showing the laminar hydathode consisting of a giant trichome, numerous salt-glandular trichomes, and a group of water pores. E, SEM micrograph showing a hydathode at leaf tip of a young leaf. F, SEM micrograph showing a mature laminar hydathode showing a trichome, a remnant salt-glandular trichome, and a group of water pores. G, SEM micrograph of a hydathode with chalk scales (arrowheads) dispersed on outer surface of leaf after the guttate fluid evaporated. H, SEM micrograph showing salt crystals (arrowhead) precipitated on outer surface of the water pores. I, SEM micrograph showing fungal mycelia (arrowhead) growing on the outer surface of a hydathode. Some of them are even intruding into the inner parts of the hydathode through the water pore. (Bar scales: A = 1 cm; B = 0.3 mm; C = 1 mm; D-G and I = 100 μm; H = 10 μm)

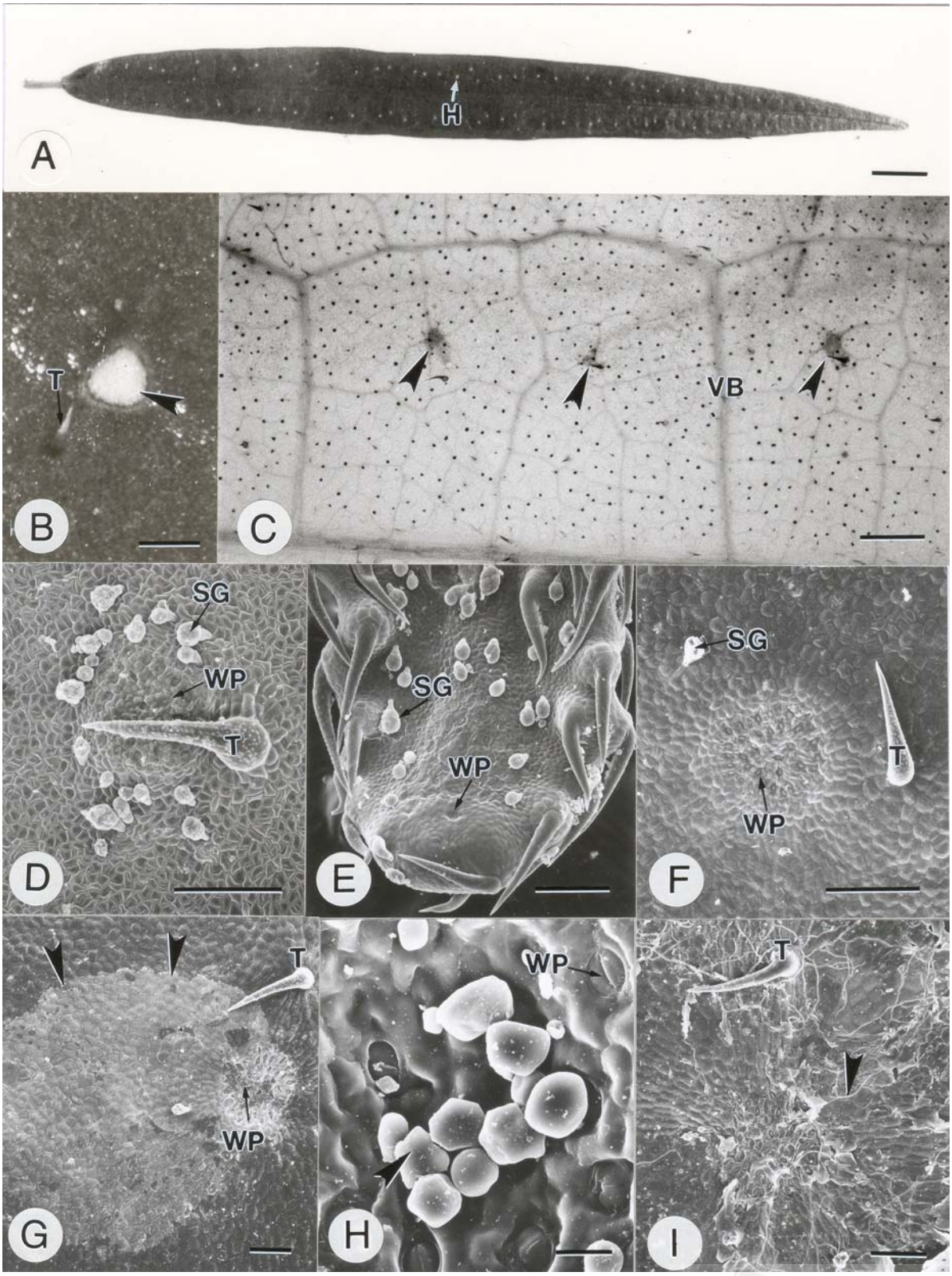

Figure abbreviations: C, chloroplast; CW, cell wall; E, epithem cell; ER, endoplasmic reticulum; G, Golgi body; H, hydathodes; IS, intercellular space; L, laticifer cell; M, mitochondrion; Mt, microtubule; N, nucleus; O, water pore aperture; P, peroxisome; PD, plasmodesmata; PT, palisade tissue; S, starch; SG, salt-glandular trichome; SL, sheath layer; ST, spongy tissue; T, trichome; TC, tracheid cell; V, vacuole; VB, vascular bundle; WP, water pore. Same abbreviations are used for all figures except Figure 2.

dular trichomes on the young leaf's surface (Figures 1D-E). The giant trichome grows well and protects the formation of hydathodes during their development. In later developmental stages, those giant and salt glandular trichomes drop off one by one in order to exclude excessive salts from the leaves (Figure 1F). White "chalk scales" are conspicuous when the xylem sap containing salt ions was guttated and evaporated (Figure 1G). These salt ions could be crystallized and precipitated into salt incrustations outside the water pores (Figure 1H). Moreover, the guttated fluid is rich in nutrients. Sometimes, different kinds of fungi growing on the surface of hydathodes can be observed, and they can even grow through the water pore into the hydathode's inner parts (Figure 1I).

The hydathode number per leaf and leaf-length share a positive correlation, based on our measurement of 190 leaves from 15 shoots. Their correlation coefficient is 0.66 (Figure 2). The hydathode distribution per centimeter of leaf-length on the leaf adaxial surface averages 3 to 4. In addition, each hydathode contains 30 to 60 water pores.

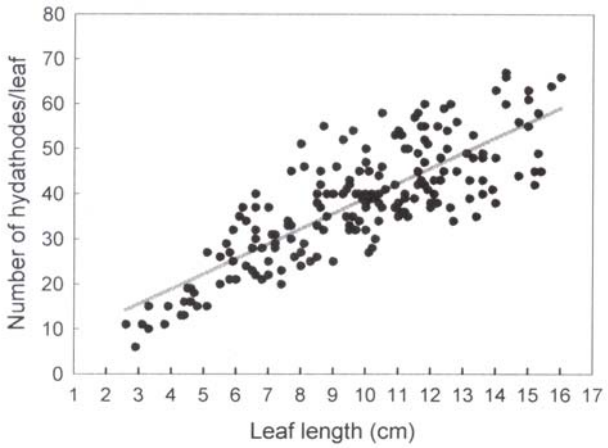

Figure 2. Correlation between the number of hydathodes per leaf and leaf length of 190 leaves from 15 shoots of *F. formosana* Maxim. f. *Shimadai* Hayata plants. The regression is Y = 3.356 X + 5.455 (n = 190, r^2 is 0.66, $p<0.05$). X is the leaf-length, and Y is the number of hydathodes per leaf.

Anatomy of Laminar Hydathode, Investigated by Light Microscopy

To illustrate the structure of the laminar hydathodes, we used light microscopy to examine leaf cross-sections and different paradermal sections (Figure 3). Laminar hydathodes consist of epidermis, water pores, and the epithem. The epithem is made up of a group of conspicuous lobed cells surrounded by a sheath layer (Figure 3A). The three-dimensional relationships among the different elements in a hydathode are shown as follows: 1. The adaxial outer surface of leaf has water pores dispersed among the epidermal cells (Figure 3B); 2. Beneath the epidermis, a roomy intercellular space is contact with the epithem, which consists of a group of sinuous cells surrounded by a sheath layer (Figures 3A, C); 3. Four vascular bundles in different directions are joined up into the epithem (Figure 3D). The water pore passes through two guard cells. A sheath layer with elongated parenchyma cells, surrounding epithem cells, and tracheid element junction extends from the epithem bottom to the epidermis.

Laticifers are distributed throughout the leaf. They are often seen extending to bend and branch around, sometimes even to the boundary of the hydathodes. It is noteworthy that laticifers somehow never intrude into the hydathodes (Figures 3C, D).

Ultrastructure of Laminar Hydathode, Investigated by TEM

As shown in Figure 4A, the water pores pass through two guard cells. The outer ridges of these cells are overlapped, and their structure resembles an observatory tower. They are opened under the high hydrostatic pressure over the threshold value, and the middle part of the inside pore is permanently opened. Beneath the water pores, sits a spacious intercellular chamber on the upper part of the epithem. In Figure 4B, the water pore has two irregular guard cells paired with a small pore between them. The guard cell is not kidney-shaped and is different from the ordinary stomata, which is on the hypodermis for gas exchange.

The epithem cells have successive sinuous cell walls and conspicuous intercellular spaces that provide larger surface-contact area between the epithem cells and xylem saps (Figure 4C). Epithem cells contain a dense cytoplasm rich in ribosomes, numerous mitochondria, small chloroplasts, many obvious proliferate peroxisomes, and several large vacuoles acompanied by small vesicles. In addition, abundant plasmodesmata can be noted between the two epithem cells (Figures 4D, E). Microtubules occur near the wall protuberance regions of the lobed cell (Figure 4F). The chloroplasts within the epithem are small in size, have no conspicuous thylakoid membranes or grana, and are different from the mesophyll cells (Figures 4C, G). The peroxisomes, mitochondria, and chloroplasts in connection with each other are frequently observed (Figure 4G). Abundant Golgi bodies and ER membranes are associated with many small vesicles with dense contents, and they appear in cytoplasm regions near the sinuous cell wall (Figure 4H). A sheath layer surrounding the epithem is extended from bottom of epithem to epidermis. The cytological characteristics of sheath layer cells are that a large central vacuole presents itself in the side-facing epithem and that most organelles in cytoplasm are packed on the side away from the epithem (Figure 4I). Plasmodesmata are present between the epithem cell and sheath layer cells (data not shown).

Variable Morphology of Plasmalemmasome

In addition to the generally occurring organelles, endocytosis appeared to have added some membrane-bounded granular structures, perhaps the result of plasmalemma invagination. The endocytic vesicle structures are in different shapes, and are uncovered in the

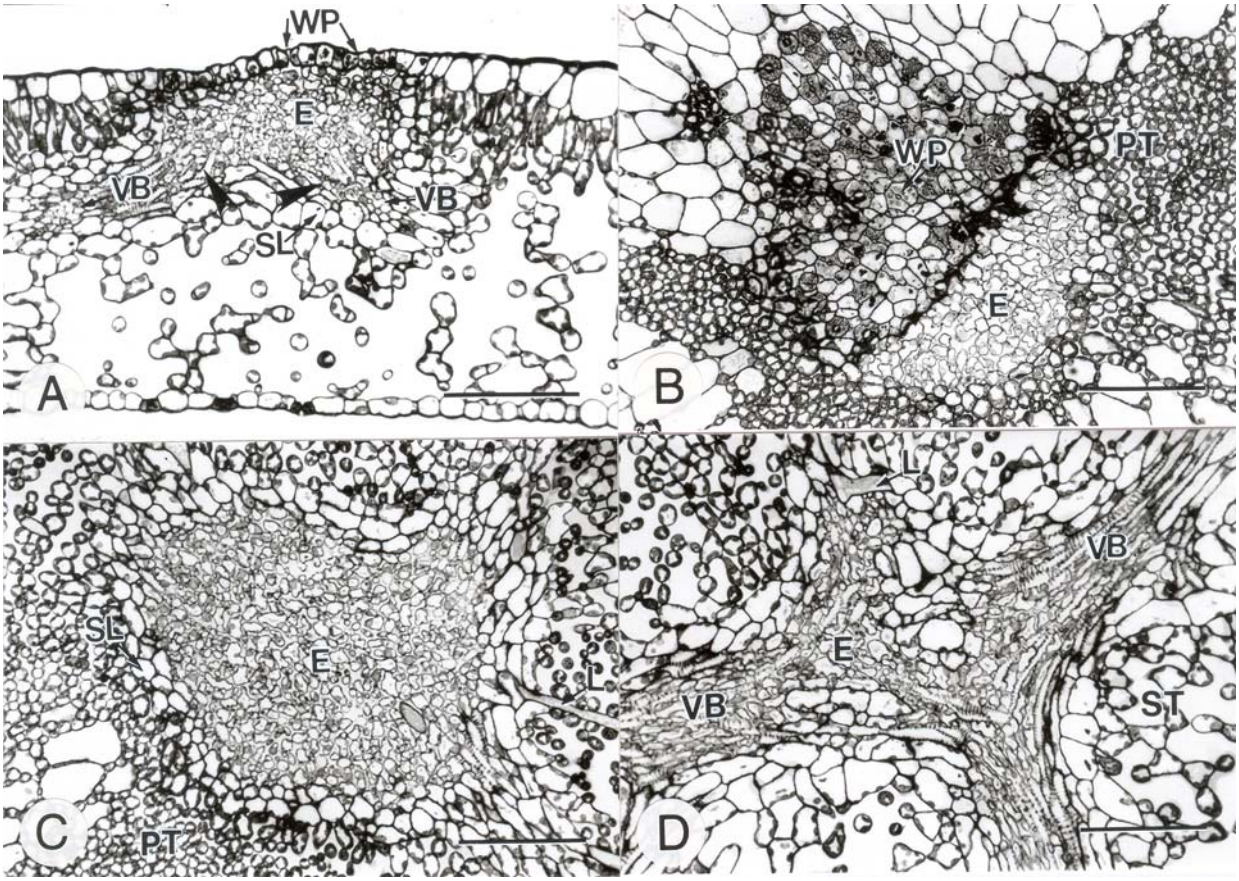

Figures 3A-D. Light micrographs of cross and paradermal sections of the leaf showing a laminar hydathode in *F. formosana* Maxim. f. *Shimadai* Hayata. A, Resin-embedded cross-section of a hydathode. Outer surface consisted of epidermis and water pores; inside region included the epithem consisting of a group of small lobed cells, two vascular bundles extending upward (arrowheads), and a sheath layer surrounding the tracheid elements, and the epithem then extends to the epidermis. B, Oblique paradermal section of the hydathode through the epidermis level showing the vicinity of a hydathode consisting of water pores and epidermis cells. C, Paradermal section of a hydathode through the middle level of epithem showing the epithem consisting of a group of small lobed parenchyma cells and surrounded by a sheath layer. D, Paradermal section of a hydathode through the vascular bundle level showing four vascular bundles and their tracheid element junction under the epithem. (All bar scales = 50 μm).

plasma membrane regions (Figures 5, 6). The above structures are located within the epithem as follows: in the region of contacting surface between epithem cells (Figure 5D), on the margin facing tracheids or intercellular spaces (Figures 6A-C), and in the plasmodesmata regions between epithem cells (Figure 6D). As shown in Figures 5E-F, various plasmodesmata are present between epithem cells, and many polyribosomes are distributed throughout the pericytoplasm. Mild salt and osmotic stresses cause the plasmalemma of the epithem cells to shift from wavy to tubular membrane invagination (Figures 5A-D). Heavier osmotic shock can induce more plasmalemma invagination through small vesicles to form a larger vacuolar body (Figure 6). Corresponding to different stress levels, the vesicular bodies appear in various morphologies (Figures 6A-F). In addition, some resembling structures also occur in the epidermis adjacent to water pores, but have larger vesicles within the vesicular body (Figure 6G). Figures 6H and 6I show the two successive processes of the fluid-phase endocytosis in the epithem cells. Plasmalemmasomes appear with small vesicles inside the pre-invagination of plasmalemma and move toward the tonoplast for the formation of a larger vesicle (Figure 6H). After the fusion of plasmalemma, the tonoplast has yet to merge (Figure 6I). Accordingly, after the fusion of tonoplast the vesicular bodies are transferred into the vacuole.

Discussion

Type of Laminar Hydathode of F. formosana; Typical Illustration of Epithemal Hydathode

The laminar hydathodes of *F. formosana* Maxim. f. *Shimadai* Hayata is a typical epithemal hydathode and consists of water pores, epithem, tracheid elements, and a sheath layer. The occurrences of the hydathodes are close around the leaf venation, especially presented above the junction of the tracheid elements. Such compositions are classified as complex epithemal hydathodes, which are different from the leaf-tip's epithemal hydathodes of grass, a reduced form (Maeda and Maeda, 1987, 1988; Dieffenbach et al., 1980).

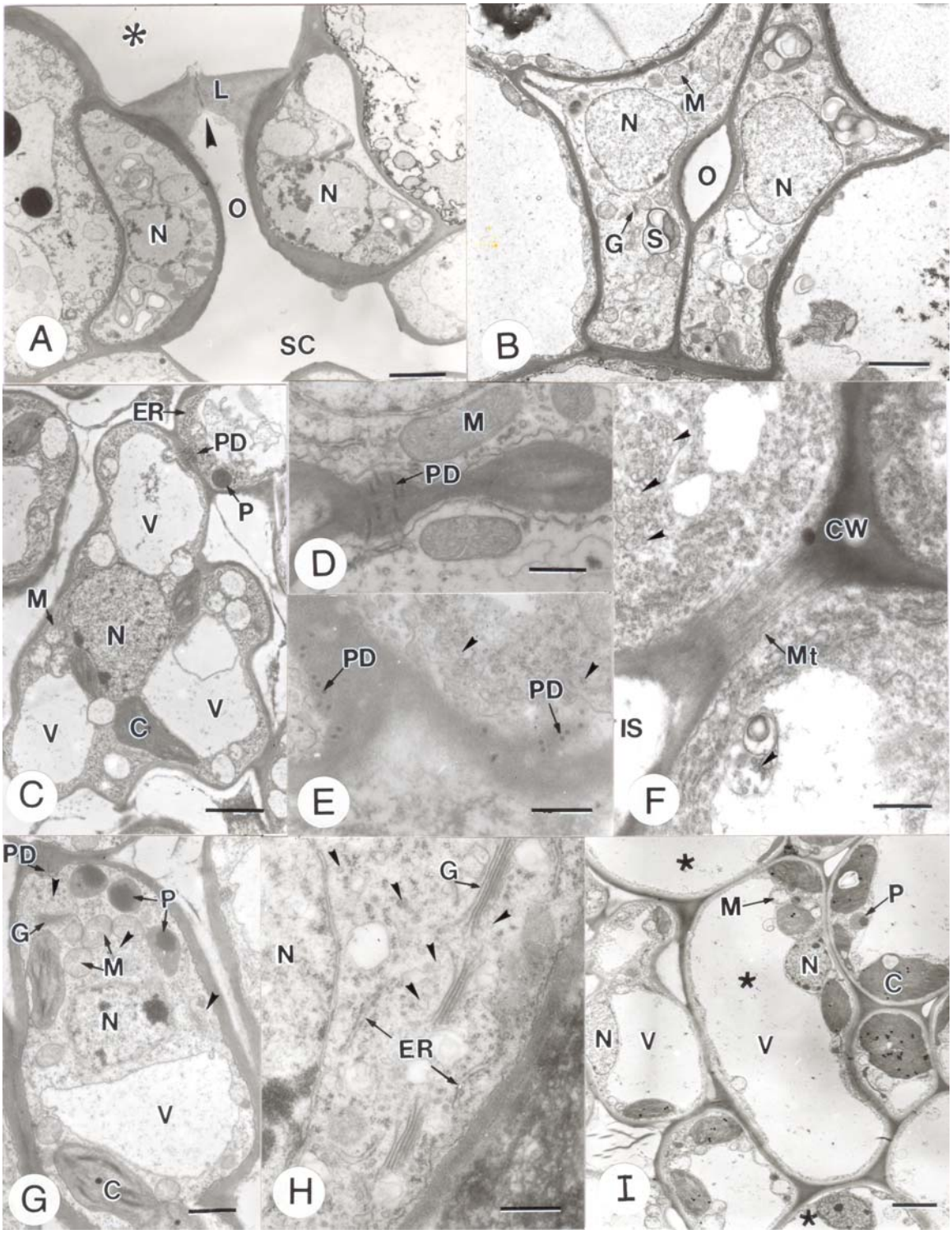

Figures 4A-I. Ultrastructures of laminar hydathodes in *F. formosana* Maxim. f. *Shimadai* Hayata. A, TEM micrograph showing cross-section of the water pore on leaf adaxial surface. The water pore is externally covered by two overlapping ridges of modified guard cells (arrowhead). Asterisk indicates the outside environment. B, TEM micrograph showing paradermal section of the water pore with two modified guard cells. The aperture is permanently opened (O). C, TEM micrograph of epithem cell with conspicuous sinuous cell wall, vacuoles, peroxisomes, mitochondria, and abundant plasmodesmata between epithem cells. D, Magnification of longitudinal-section of plasmodesmata. E, Magnification of cross-section of plasmodesmata. Arrowheads indicate vesicles. F, TEM micrograph showing microtubules present near the periplasmic region of tortuous cell wall. Arrowheads indicate vesicles. G, Magnification of an epithem cell showing different organelles including a nucleus, peroxisomes, mitochondria, and chloroplasts. Arrowheads indicate vesicles. H, Magnification of partial epithem cell showing three Golgi bodies, ER and many vesicles (arrowheads). I, TEM micrograph of sheath layer cells with a large central vacuole, and most of organelles and cytoplasm distributed far from near epithem side. Stars indicate the sheath layers. (Bar scales: A-C and I = 2.5 μm; D-F = 0.5 μm; G = 1.25 μm; H = 0.25 μm)

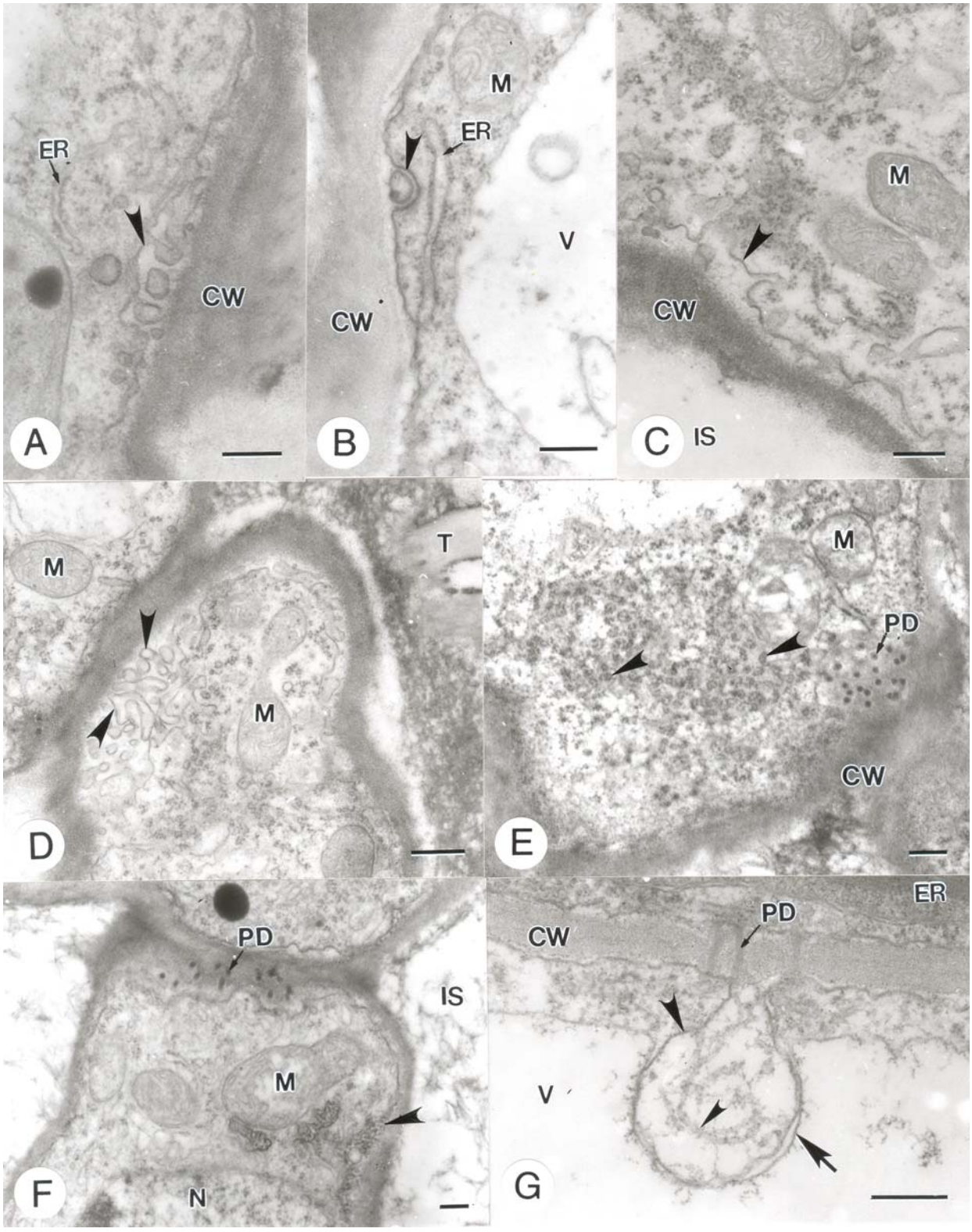

Figures 5A-G. Ultrastructure of plasma membranes present in epithem cells. A, TEM micrograph of reticular invagination of plasma membrane to form paramural bodies (arrowhead). B, TEM micrograph showing tubular invagination of plasma membrane (arrowhead). C, TEM micrograph of loose and tortuous plasma membrane (arrowhead). D, TEM micrograph showing the incipient of anomalous vesicular formation (arrowheads) at plasma membrane of epithem cells. E, TEM micrograph showing a group of plasmodesmata and a lot of polyribosomes (arrowheads) in pericytoplasm. F, TEM micrograph showing reticulated invagination of the plasma membrane (arrowhead). G, TEM micrograph showing invagination of plasma membrane nearby plasmodesmata between two epithem cells. A small arrowhead indicates the tubular materials occurring in the endocytic vesicle. A large arrowhead indicates the plasma membrane, and arrow indicates the tonoplast membrane. (All bar scales = 0.25 μm).

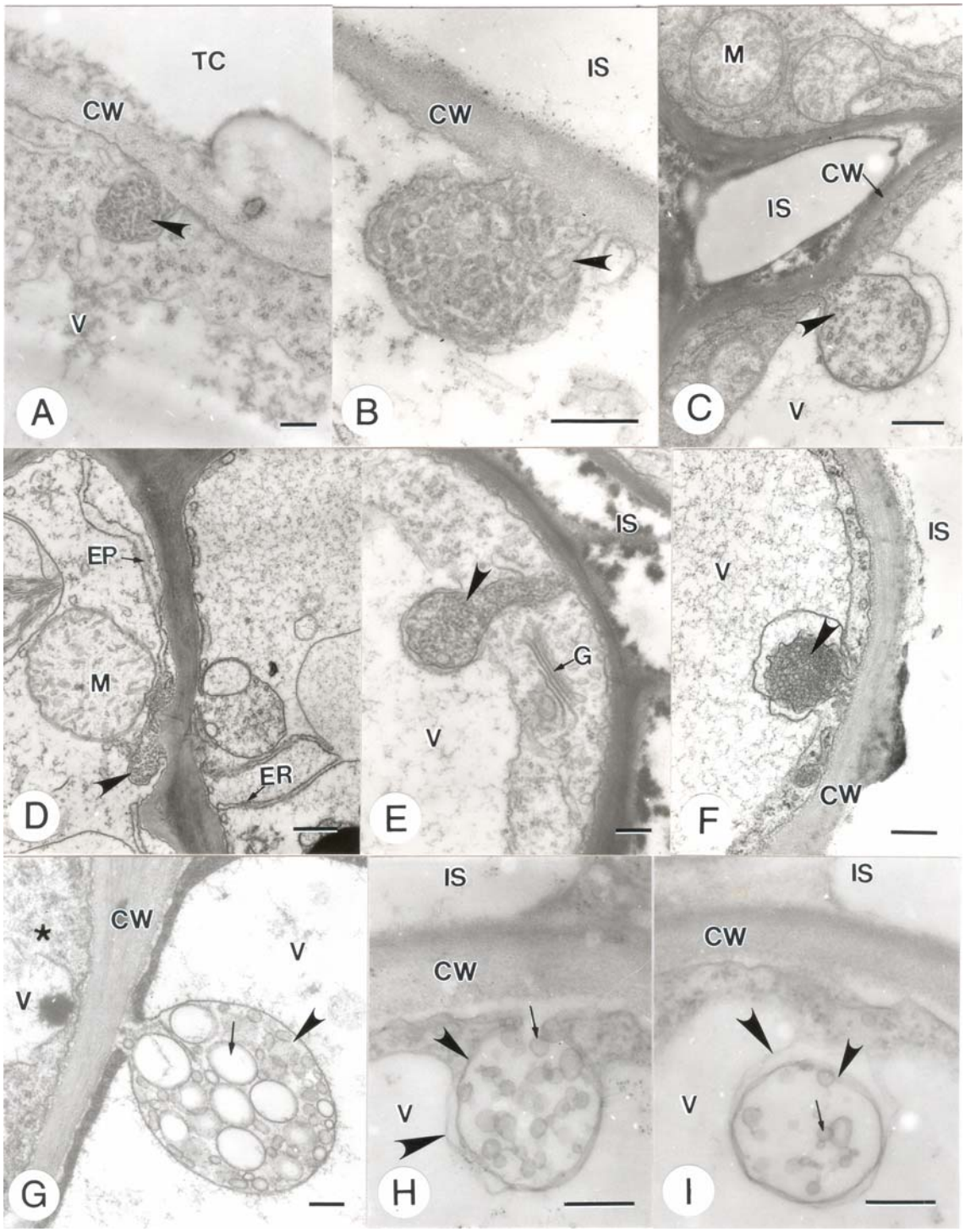

Figures 6A-I. Multi-shapes of the plasma membrane during fluid-phase endocytosis occurring in hydathodes. A, TEM micrograph showing the reticulated type of plasmalemmasome (arrowhead) observed in the epithem cell facing the tracheid cell. B, TEM micrograph showing the reticulated type of plasmalemmasome (arrowhead) occurring in the epithem cell facing intercellular space of hydathodes. C, TEM micrograph of fluid-phase endocytosis occurring in the epithem cell. The arrowhead indicates the endocytic vesicle. D, TEM micrograph of plasmalemmasome (arrowhead) near plasmodesmata between two epithem cells. E, F, TEM micrographs showing two types of endocytosis performed in epithem cell facing the intercellular space of hydathodes. A multivesicular body (arrowhead) is formatted and directing the protrusion into the vacuole. G, TEM micrograph of fluid-phase endocytosis occurring in epidermal cell of hydathodes. A multivesicular body (arrowhead) and many large vesicles (arrow) are observed in epidermis, and the opposite cell is the water pore cell (star). H, I, TEM micrographs showing the two processes of fluid-phase endocytosis found in the epithem cells. The endocytosis in Figure H occurs earlier than that of Figure I, where the vesicle is formed and finally bogged into the vacuole. Arrow indicates the small vesicle, a small arrowhead the plasma membrane, and a large arrowhead the tonoplast membrane. (All bar scales = 0.25 μm).

Functions of Salt-glandular Trichomes and Non-glandular Trichome

There are many salt-glandular trichomes surrounding the surface area of the laminar hydathode during the early period of hydathode development. The number of salt-glandular trichomes tapers off during the maturation of hydathode. The function of these salt-glandular trichomes is believed to be to exclude excessive salt ions that are supposed to keep ion homeostasis in association with salt tolerance (Thomson, 1975). In general, a giant trichome plays an important role in plant defense, particularly with regard to phytophagous insects (Levin, 1973). Overall, we suggested that these trichomes in the vicinity of hydathodes provide protection in the early developmental stage while the dropping of the glandular trichomes at the mature stage could actively eliminate salt ions from xylem saps.

Salt Incrustation Formation and Pathogen Infection

The guttation drops on a plant have three possible fates. They may roll off, be evaporated, or be sucked into the leaf, as most frequently happen on undisturbed plants (Curtis, 1943). When guttate solution evaporates in the daylight, salt incrustations can be precipitated around the vicinity of the surface of hydathodes. Because guttate fluid is rich in nutrients for microbial growth, several bacterial cells and fungal hypha growing near hydathodes have often been noticed. Hydathodes have been found to serve as an extremely efficient infection court for the bacterial pathogen (Dane and Shaw, 1993; Carlton et al., 1998; Fukui et al., 1999) and as a practical system for studying early infection events in bacterial pathogenesis (Hugouvieux et al., 1998).

In addition, epithem cells have dense cytoplasm, numerous mitochondria, extended ER systems, and a considerable numbers of small vesicles within the cytoplasm. The epithem cells could modify the content of the guttate fluid along the transport route and indirectly affect the composition of salt incrustation (Dieffenbach et al., 1980).

Polar Distribution of Organelles in the Sheath Layer

Figure 4I shows that the sheath layer cell has a big central vacuole occupying most of the cell's space that pushes the nucleus and other organelles along with the cytoplasm forward to the opposite side of epithem. At the same time, many plasmodesmata are present not only between the epithem and sheath layer cell, but also between the sheath layer cells (data not shown). Plasmodesmata connected with each other seem to increase the transport efficiency between different epithem cells and/or cells of the sheath layer (Epel, 1994; Lucas, 1995; Cantrill et al., 1999; Crawford and Zambryski, 1999). The polar distribution of organelles lets the central vacuole nearly contact the epithem cells which might reduce the transport material carried into the vacuole through cytoplasm and also increase its transport efficiency.

Sinuous Cell Wall of Epithem Increasing Surface of Absorption

In this study, we have observed that the epithem cells are lobed in shape. The sinuous cell wall can increase the contact surface area between the cell wall and xylem sap, which can improve the absorption rate of epithem cells (Sattelmacher, 2001). According to the studies of Komis et al. (2002), hyperosmotic stress can induce the reorganization of actin filaments in leaf cells of *Chlorophyton comosum*. The question arises whether the osmotic pressure induces a special epithemal ontogenesis through the rearrangement of microtubules or actin filaments. A further study to resolve this is needed.

Endocytosis in Epithem Cells

It is interesting that the plasma membrane of epithem cell is very unstable after transpiration. The transpiration triggers increase of the solute concentration in xylem sap within hydathodes that cause high salt and high osmotic conditions in the epithem cell. These stresses can affect the morphology of the plasmalemma. Through the study of variability of plasmalemmosomes in epithem cells, we suggested that particular structures might be a result of the membrane invagination of epithem cells under high salt and osmotic stress (Gordon-Kamm and Steponkus, 1984; Oparka et al., 1990). At the same time, the sinuous cell walls of the epithem cells have the potential to propose the enlargement of membrane surfaces to regulate a unique membrane area/cell volume ratio. Especially, repetition of guttation and transpiration cycles induces solute concentration change and let epithem cells undergo plasmolysis and deplasmolysis cycles, making fluid-phase endocytosis more likely (Oparka et al., 1990).

Regarding the membrane invagination of endocytosis, Nishizawa and Mori (1977, 1978) investigated the entry mechanism of organic nitrogen into rice root cells using electron microscopy. Many invaginations of the plasmalemma were observed in the differentiating and elongating zone of the roots and could be classified tentatively into three types. They suggested that endocytosis occurred in rice root cells. In our study, the variability of plasmalemmasome occurred in the epithem cell, which is consistent with the observation of Nishizawa and Mori. In other words, hydathode may be an ideal system, besides the root system, for studying endocytosis in plants.

Literature Cited

Brouillet, L., C. Bertrand, A. Cuerrier, and D. Barabe. 1987. Les hydathodes des genres *Begonia* et *Hillebrandia* (Begoniaceae). Can. J. Bot. **65:** 34-52.

Cantrill, L.C., R.L. Overall, and P.B. Goodwin. 1999. Cell-to-cell communication via plant endomembranes. Cell Biol. Int. **23:** 653-661.

Carlton, W.M., E.J. Braun, and M.L. Gleason. 1998. Ingress of *Clavibacter michiganensis* subsp *michiganensis* into tomato leaves through hydathodes. Phytopathology **88:** 525-529.

Crawford, K.M. and P.C. Zambryski. 1999. Plasmodesmata

signaling: many roles, sophisticated statutes. Curr. Opin. Plant Biol. **2:** 382-387.

Curtis, J.D. and N.R. Lersten. 1974. Morphology, seasonal variation, and function of resin glands on buds and leaves of *Populus deltoids* (Salicaceae). Amer. J. Bot. **61:** 835-845.

Curtis, L.C. 1943. Deleterious effects of guttated fluid on foliage. Amer. J. Bot. **30:** 778-781.

Dane, F. and J.J. Shaw. 1993. Growth of bioluminescent *Xanthomonas-campestris* pv. *campestris* in susceptible and resistant host plants. Mol. Plant-Microbe Interact **6:** 786-789.

Dieffenbach, H., D. Kramer, and U. Lüttge. 1980. Release of guttation fluid from passive hydathodes of intact barley plants. I. Structural and cytological aspects. Ann. Bot. **45:** 397-401.

Elias, T.S. and H. Gelband. 1977. Morphology, anatomy, and relationship of extrafloral nectarines and hydathodes in two species of impatiens (Balsaminaceae). Bot. Gaz. **138:** 206-212.

Epel, B.L. 1994. Plasmodesmata: composition, structure and trafficking. Plant Mol. Biol. **26:** 1343-1356.

Fahn, A. 1979. Secretory Tissues in Plants. Academic Press, London.

Fukui, R., H. Fukui, and A.M. Alvarez. 1999. Suppression of bacterial blight by a bacterial community isolated from the guttation fluids of anthuriums. Appl. Environ. Microbiol. **65:** 1020-1028.

Gordon-Kamm, W.J. and P.L. Steponkus. 1984. The behavior of the plasma membrane following osmotic contraction of isolated protoplasts: implications in freezing injury. Protoplasma **123:** 83-94.

Haberlandt, G. 1914. Physiological Plant Anatomy, Engl. Trans. London.

Hugouvieux, V., C.E. Barber, and M.J. Daniels. 1998. Entry of *Xanthomonas campestris* pv. *campestris* into hydathodes of *Arabidopsis thaliana* leaves: A system for studying early infection events in bacterial pathogenesis. Mol. Plant-Microbe Interact. **11:** 537-543.

Komis, G., P. Apostolakos, and B. Galatis. 2002. Hyperosmotic stress-induced actin filament reorganization in leaf cells of *Chlorophyton comosum*. J. Exp. Bot. **53:** 1699-1710.

Kramer, P.J. 1945. Absorption of water by plants. Bot. Rev. **11:** 310-355.

Lepeschkin, W.W. 1923. Über active und passive Wasserdrusen und Wasserspalten. Ber. Deut. Bot. Ges. **41:** 298-300.

Lersten, L.R. and J. D. Curtis. 1982. Hydathodes in *Physocarpus* (Rosaceae: Spiraeoideae). Can. J. Bot. **60:** 850-855.

Lersten, L.R. and J. D. Curtis. 1985. Distribution and anatomy of hydathodes in Asteraceae. Bot. Gaz. **146:** 106-114.

Lersten, L.R. and J.D. Curtis. 1991. Laminar hydathodes in Urticaceae: survey of tribes and anatomical observation on *Pilea pumila* and *Urtica dioica*. Pl. Syst. Evol. **176:** 179-203.

Lersten, L.R. and W. H. Peterson. 1974. Anatomy of hydathodes and pigment disks in leaves of *Ficus diversifolia* (Moraceae). Bot. J. Linn. Soc. **68:** 109-113.

Levin, D.A. 1973. The role of trichomes in plant defense. Q. Rev. Biol. **48:** 3-15.

Lucas, W.J. 1995. Plasmodesmata: intercellular channels for macromolecular transport in plants. Curr. Opin. Cell Biol. **7:** 673-680.

Maeda, E. and K. Maeda. 1987. Ultrastructural studies of leaf hydathodes. I. Wheat (*Triticum aestivum*) leaf tips. Japan. J. Crop Sci. **56:** 641-651.

Maeda, E. and K. Maeda. 1988. Ultrastructural studies of leaf hydathodes II. Rice (*Oryza sativa*) leaf tips. Japan. J. Crop Sci. **57:** 733-742.

Molisch, H. 1916. Beiträge zur Mikrochemie der Pflanze. Nr.2: über orangefarbige Hydathoden bei *Ficus javanica*. Ber. Dt. Bot. Ges. **34:** 66-69.

Nishizawa, N. and S. Mori. 1977. Invagination of plasmalemma: Its role in the absorption of macromolecules in rice roots. Plant Cell Physiol. **18:** 767-782.

Nishizawa, N. and S. Mori. 1978. Endocytosis (heterophagy) in plant cells: involvement of ER and ER-derived vesicles. Plant Cell Physiol. **19:** 717-730.

Oparka, K.J., D.A.M. Prior, and N. Harris. 1990. Osmotic induction of fluid-phase endocytosis in onion epidermis cells. Planta **180:** 555-561.

Pedersen, O., L.B. Jorgensen, and K. Sand-Jensen. 1997. Through-flow of water in leaves of a submerged plant is influenced by the apical opening. Planta **202:** 43-50.

Rost, T.L. 1969. Vascular pattern and hydathodes in leaves of *Crassula argentea* (Crassulaceae). Bot. Gaz. **130:** 267-270.

Sattelmacher, B. 2001. Tansley review no. 22 - The apoplast and its significance for plant mineral nutrition. New Phytol. **149:** 167-192.

Shobe, W.R. and N.R. Lersten. 1967. A technique for clearing and staining gymnosperm leaves. Bot. Gaz. **128:** 150-152.

Smith, D.L. and W.M. Watt. 1986. Distribution of lithocyts, trichomes, hydathodes and stomata in leaves of *Pilea cadierei* Gagnep. & Guill. (Urticaceae). Ann. Bot. **58:** 155-166.

Sperry, J.S. 1983. Observations on the structure and function of hydathodes in *Blechnum lehmannii*. Amer. Fern J. **73:** 65-72.

Spurr, A.R. 1969. A low-viscosity epoxy resin embedding medium for electron microscopy. J. Ultrastruct. Res. **26:** 31-43.

Thomson, W.W. 1975. The structure and function of salt glands. *In* A. Poljakoff-mayber and J. Gale (eds.), Plant and Saline Environments (Ecological Studies vol. 15), Springer, Berlin, pp. 118-146.

Tucker, S.C. and L.L. Hoefert. 1968. Ontogeny of the tendril in *Vitis vinifera*. Amer. J. Bot. **55:** 1110-1119.

細葉天仙果葉部泌水器的研究：I. 外部形態與超顯微構造

陳淇釧　陳榮銳

國立台灣大學分子與細胞生物學研究所

本研究以透明法、光學顯微鏡、掃描式與穿透式電子顯微鏡觀察細葉天仙果葉部泌水器的形態與超顯微構造。形態上，細葉天仙果葉部泌水器屬於複雜末梢型泌水器；它是由許多水孔與表皮細胞、管胞末端、末梢組織細胞與束鞘細胞層所組成。水孔由兩個似保衛細胞所組成，孔口屬於永久開口不具調控功能，平時是靠外脊重疊造成關閉，泌溢進行是等木質部內的靜水壓力達到臨界門檻值才推開脊口進行泌溢；末梢組織是由一群具迂迴彎曲細胞壁的薄壁細胞組成。其超顯微構造特徵是末梢細胞具有濃密細胞質、多數量的粒線體、發達內質網系統與許多衍生自高爾基氏體的小泡構造以及伴隨著末梢細胞成熟度而增殖的過氧小體。此外，末梢細胞彼此細胞壁間存有豐富的原生質連絡絲；並在末梢細胞其細胞膜內側發現許多具特別形態的細胞膜內凹體，這些細胞膜內凹體是由於不斷重複的細胞質離與去質離作用所造成細胞膜內噬作用而形成的構造。我們認為泌水器可提供為日後研究植物細胞膜內噬作用的一個理想研究系統。

關鍵詞：內噬作用；末梢組織；細葉天仙果；葉部泌水器；細胞膜內凹體；超顯微構造；水孔。